Magic Monatomic Linear Chains for Mn Nanowire Self-Assembly on Si(001)

Jian-Tao Wang,[1,2,*] Changfeng Chen,[2] Enge Wang,[3] and Yoshiyuki Kawazoe[4]

[1]*Beijing National Laboratory for Condensed Matter Physics, Institute of Physics, Chinese Academy of Sciences, Beijing 100190, China*

[2]*Department of Physics and HiPSEC, University of Nevada, Las Vegas, Nevada 89154, USA*

[3]*International Center for Quantum Materials, School of Physics, Peking University, Beijing 100871, China*

[4]*Institute for Materials Research, Tohoku University, Sendai, 980-8577, Japan*

(Received 5 May 2010; published 8 September 2010)

Using first-principles calculations, we unveil an atomistic nucleation process of monoatomic Mn nanowire self-assembly on Si(001). We find that Mn adatoms form magic $3n + 1$ atom dense trimerlike linear chains (DTLCs) driven by pedestal site adsorption. Moreover, the length of DTLCs is limited by a competing process to form three-dimensional D_{3h}-Mn_5 clusters in early stages. These results establish a new structural model distinct from the dimerlike linear chains for III and IV group elements on Si(001) and provide a natural explanation for recent experimental observations.

DOI: 10.1103/PhysRevLett.105.116102 PACS numbers: 68.43.Mn, 68.43.Bc, 68.43.Jk, 75.75.−c

There has been considerable interest in recent years in manganese and manganese silicide as promising candidates for spintronics applications [1–3]. In particular, the study of the initial stages of the growth of Mn on Si(001) is most important in the context of the possibility to fabricate magnetic heterostructures of Mn-Si and related compounds by molecular-beam epitaxy. Scanning tunneling microscopy (STM) studies [3] reveal that room temperature deposition leads to preferential formation of monoatomic Mn wires in early stages, and small clusters appear at higher coverage and compete with the wire growth. Previous theoretical studies on the growth mechanism of Mn on Si(001) [4–10] and Ge(001) [11] have mainly focused on the surface diffusion of a single Mn atom. The more complicated and important atomistic nucleation processes in the early stages of Mn nanostructure formation on Si(001) remain largely unexplored, which hinders the determination of the positions of Mn atoms within the nanowires with respect to the Si surface [3]. Understanding the precise nature of Mn adsorption sites, the bonding to the Si surface and the growth mechanism of the nanowire structures is critical to predicting and tailoring Mn-Si nanostructure properties.

In this Letter, we present a comprehensive study of the energetics and kinetics for the formation of monoatomic linear chains of Mn on Si(001) using first-principles total-energy calculations. We find that Mn adatoms on Si(001) prefer forming finite dense trimerlike linear chains (DTLCs) with magic number of $3n + 1$ Mn atoms aligned perpendicular to the surface dimer rows. It is distinct from the dimerlike linear chain formation for III and IV group elements on Si(001). The diffusion of Mn adatoms on Si(001) encounters only small energy barriers of $\sim$0.50 eV for diffusing both perpendicular to and along the substrate dimer rows. As a result, Mn adatoms can easily diffuse into the favorable positions to form the magic one-dimensional DTLCs. Meanwhile, the length of a DTLC is limited by a competing process to form three-dimensional D_{3h}-Mn_5 clusters on Si(001).

The calculations are carried out using the Vienna *ab initio* simulation package (VASP) [12] with the projector augmented wave method [13] and spin-polarized generalized gradient approximation [14] for the exchange-correlation energy. The valence states $3p^6 3d^5 4s^2$ for Mn and $3s^2 3p^2$ for Si are used with an energy cutoff of 320 eV for the plane wave basis set and a cutoff of 570 eV for the augmentation charges. Our calculations obtained the bulk lattice constant of 3.865 Å for Si, in good agreement with the experimental value of 3.84 Å. For the surface calculations, we use a supercell $XYZ = 15.46$ Å $\times$ 15.46 Å $\times$ 27 Å with a 4×4 unit cell in the XY plane and eight layers of silicon in the Z direction. The clean surface has a $p(2 \times 2)$ symmetry in agreement with the experimental observation [3]. One layer of hydrogen is set to passivate the back surface of the Si substrate with a vacuum layer of about 16 Å in the Z direction. Two bottom Si layers are fixed at the bulk structure, while the other Si and Mn atoms are fully relaxed. The energy minimization is done over the atomic and electronic degrees of freedom using the conjugate gradient iterative technique. The Brillouin zone is sampled using the k point at $L(1/2, 1/2, 1/2)$ as in Ref. [8]. Convergence criteria employed for both the electronic self-consistent relaxation and the ionic relaxation were set to 10^{-4} eV and 0.02 eV Å^{-1} for energy and force, respectively. To study the nucleation reaction and diffusion pathway, we employed the climbing image nudged elastic band method (CI NEB), as implemented in VASP by Henkelman, *et al.* [15]. The images of the CI NEB were relaxed until the maximum residual force was less than 0.01 eV Å^{-1}.

Figure 1 shows various optimized configurations with 1–6 Mn adatoms on Si(001) surface and their adsorption energies defined as

$$E_{\mathrm{ad}} = (E_{\mathrm{Mn/Si(001)}} - E_{\mathrm{Si(001)}} - NE_{\mathrm{Mn}})/N, \qquad (1)$$

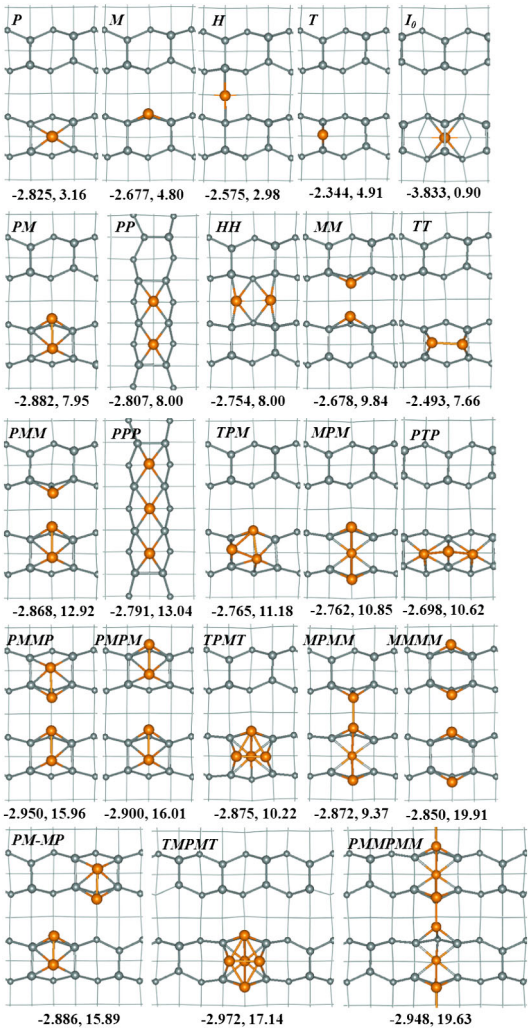

FIG. 1 (color online). Optimized configurations for ad-Mn atoms on Si(001). Large (red) and small (gray) circles represent the ad-Mn atoms and the Si atoms in the top two layers of the substrate, respectively. Lines are drawn to indicate the electronic bonds. The adsorption energies (in eV) defined in the text and magnetic moments (in μ_B) are listed below each structure.

where the first term is the total energy of the Mn/Si(001) system, the second term is that of the corresponding clean Si(001)-(2×1) surface, E_{Mn} is the total energy of one isolated Mn atom, and $N = 1$–6 is the number of Mn adatoms on Si(001). The most stable position for a single Mn adatom is the pedestal site P on the top of the substrate dimer row with four Mn-Si bonds, the same as for Mn on Ge(001) [11]; the second most stable position is on the M site along the trough between dimer rows, which is the most stable position for a Si adatom on Si(001) [16]; and the third possible position is on the hollow site H in the trough (see Fig. 2). For comparison, a top adsorption site T, located 2.04 Å above the Si dimer, is also shown with a small binding energy of 2.34 eV, in contrast to an interstitial site I_0 located 2.29 Å beneath the Si dimer with a larger binding energy of 3.83 eV. The magnetic moments for these structures are also shown in Fig. 1. Our E_{ad} and

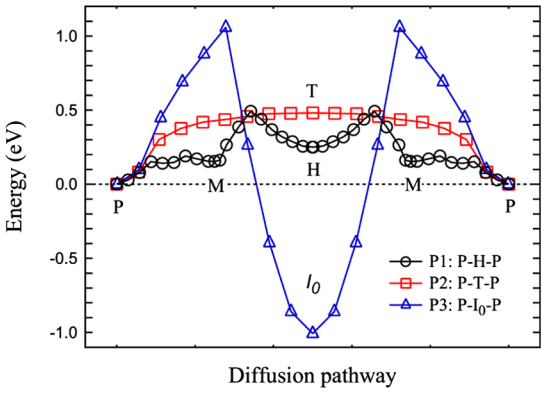

FIG. 2 (color online). Relative total energy versus the reaction pathways for ad-Mn diffusion on Si(001) surface. $P1$ ($P \rightarrow H \rightarrow P$) is a *hopping* pathway, across the dimer rows; $P2$ ($P \rightarrow T \rightarrow P$) is a *rolling-over* pathway, parallel to the dimer rows; $P3$ ($P \rightarrow I_0 \rightarrow P$) is an *insert* pathway along the surface dimer row. The typical atomic configurations are shown in Fig. 1.

magnetic moments for P and I_0 structures are consistent with previous results [7–9].

We now explore possible diffusion pathways for a single Mn adatom on Si(001). When a Mn atom adsorbs on the stable site P, three possible diffusion pathways are considered: $P1$ ($P \rightarrow H \rightarrow P$) is a *hopping* pathway, across the dimer rows [11]; $P2$ ($P \rightarrow T \rightarrow P$) is a *rolling-over* pathway, parallel to the dimer rows, and $P3$ ($P \rightarrow I_0 \rightarrow P$) is an *insert* pathway [11] along the surface dimer row. The relative energies are plotted in Fig. 2. The energy barriers are estimated to be 0.49, 0.48, and 1.06 eV for $P1$, $P2$, and $P3$, respectively. The values for $P1$ and $P2$ are close to the available data of 0.55 eV for Mn on Si(001) [7] and 0.59 eV for Mn monomer on Ge(001) [11] and the estimated insert diffusion barrier is close to the result of 0.96 eV given by Dalpian *et al.* [8]. In contrast to our result, Zhu *et al.* [11] found a small barrier, 0.69 eV, for the insert pathway of Mn on Ge(001). This difference can be attributed to the weak bonding and longer bond length between Ge-Ge and Ge-Mn on Ge(001) versus the strong bonding and shorter bond length between Si-Si and Si-Mn on Si(001). In fact, there is a bond breaking of the Si-Si dimer through the insert pathway to across the five-odd-membered ring of Si. Note that our value is indeed comparable to the diffusion barrier (1.17 eV) for a Mn impurity in bulk silicon through the path $T_d \rightarrow D_{3d} \rightarrow T_d$ across the six-membered ring [17]. These results clearly show that Mn adatoms can easily diffuse along or across the dimer rows, but are kinetically limited for diving into the subsurface layer or diffuse into the deep layer at room temperature on Si(100) [18].

We next consider the nucleation process to form a Mn wire or cluster on Si(001). In Fig. 1, we show five possible dimer or dimerlike structures PM, PP, and TT on the dimer rows and HH and MM on the trough. Here the dimers PM and TT are well defined for Si, Ge, and Bi on Si(001) [19–24], and an MM-type dimer has been used to describe the structure of group III elements Al and Ga on

Si(001) [25–27]. However, among them, only the *PM* dimer is more stable than the *P* site ad-Mn. This means that when a Mn atom is adsorbed on the surface, it can easily move along or across the dimer row, and meet together to form a *PM* dimer on a substrate dimer row. By CI NEB calculation, we find that the energy barrier to form the dimer *PM* from *P* and *H* monomers is only 0.26 eV, which is almost the same as the diffusion process $H \rightarrow M$ in the trough (see Fig. 2). However, the dissociation barrier from *PM* to *P* is estimated to be 0.60 eV. This means that the *PM* dimer is just a metastable structure dynamically.

To understand the anisotropic bonding behavior, we examine five possible trimerlike structures shown in Fig. 1. Here *PMM* and *MPM* are linear chains perpendicular to the dimer row, *PPP* and *PTP* are parallel to the dimer row, and *TPM* is a 3D cluster on the dimer row. We can see that the trimer (*PMM*) is more favorable perpendicular to the surface dimer row than that (*PPP*) parallel to the surface dimer row. This anisotropic bonding behavior can be considered as a basic feature of the formation of Mn nanowires on the Si(001) surface. Here *PMM* is more favorable than the *MPM* chain and the 3D *TPM* cluster, showing a site selective bonding nature for a new addition of Mn atom on the *PM* dimer due to the favorable dimerlike bond of *MM* over the trough. However, all the considered trimers are less stable than the dimer *PM* in energy. This means that the initial trimers are quite unstable and will further grow into a longer wire or larger cluster. To clarify this point, several possible bonding structures in a tetramer chain or 3D cluster are further explored. It is identified that the most stable tetramer is a monoatomic chain *PMMP* with a pair of connecting *PM* dimers across adjoining dimer rows. Although *MMMM* dimerlike linear chains (see Fig. 1) are favorable for Al, Ga, and Ge on Si(001) [24–27], they are less stable for Mn on Si(001), probably due to the favorable pedestal site adsorption of Mn.

It is noted that the most stable *PMMP* structure can be regarded as a short dense-linear chain (DLC), in contrast to the *PMPM* and *MMMM* dilute-linear chain structures for Mn on Si(001). Intuition suggests that an additional dimer or two adatoms may be required for constructing a dense-linear chain along the *X* direction on 4×4 surface. We indeed find a six-atom dense-linear chain with *PMMPMM* configuration, as shown in Fig. 1. In this monoatomic dense-linear chain, each $2 \times n$ unit cell contains one *P* site and two *M* site Mn atoms. Because of the induced strain along the wire stretching direction, the Mn on *P* site is pushed down into the substrate, and two *M* site Mn adatoms over the trough show a buckled dimerlike configuration with stress relief. The tilt angle of the ad-Mn dimer over the trough is about 19.62°, which is almost the same as the intrinsically buckled Si dimer (~18.4°) on the surface [24]. Also, by adding a Mn atom to the 3D *TPMT* cluster, we find a new five-atom 3D cluster *TMPMT* in D_{3h} symmetry, which is more stable than the linear chain structures shown in Fig. 1.

To understand the competing nature in the formation of the DLC and 3D clusters, finite dense trimerlike linear chains starting from an isolated Mn on the pedestal site are examined along the *X* direction on a large 8×4 surface. In Fig. 3, we plot the binding energy versus the pathways to form the dense-monoatomic Mn wires and D_{3h}-Mn_5 cluster on Si(001). We find that Mn adatoms on Si(001) prefer forming a finite DLC with magic number of $3n + 1$ $(4, 7, 10, \ldots)$, perpendicular to the surface dimer rows. They always start from and end on the *P* site, driven by the favorable pedestal site adsorption shown above. These $(3n + 1)$ magic DLCs are more stable than the *PM* dimer with a large dissociation barrier (1.12–1.28 eV for $n = 1, 2$), and their binding energies become lower monotonically as *n* increases. Meanwhile, D_{3h}-Mn_5 cluster exhibits similar energetic stability, showing the competing growth nature between the wire and 3D cluster. These results indicate that Mn clusters can occur in the early stages and coexist with the Mn wire during the growth process.

The experimentally measured height of the Mn wire is about 0.13 nm over the dimer row, which is in agreement with those of our *PMMP*, *PMPM*, *MMMM* tetramer chains and $(3n + 1)$ DLCs. On the other hand, the observed apparent height of clusters is 0.18–0.22 nm, which is in agreement with our structures of *T*, 2-*TT*, 3-*PTP*, 4-*TPMT*, and 5-*TMPMT* with one *T* or *TT* Mn on the Si dimer. Based on these results, we assign 3D 5-*PMPMT* cluster and $(3n + 1)$ dense trimerlike linear chains for the clusters and nanowires observed by Liu and Reinke [3], respectively, because they are highly stable in energy. The early stage length distribution of Mn wires seen in experiments is in the length range of 3–7 surface units, which corresponds to the magic $3n + 1$-atom dense-linear chains.

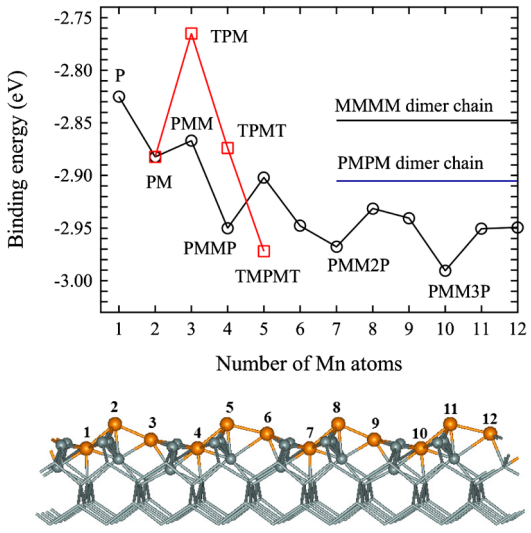

FIG. 3 (color online). Atomic binding energy versus the pathways to form a monoatomic Mn- wire (circles) or cluster (squares) on Si(001). The energies for dimerlike linear chain *PMPM* and *MMMM* are also shown for comparison. The relative structures are shown in Fig. 1. *PMM3P* = *PMMPMMPMMP*.

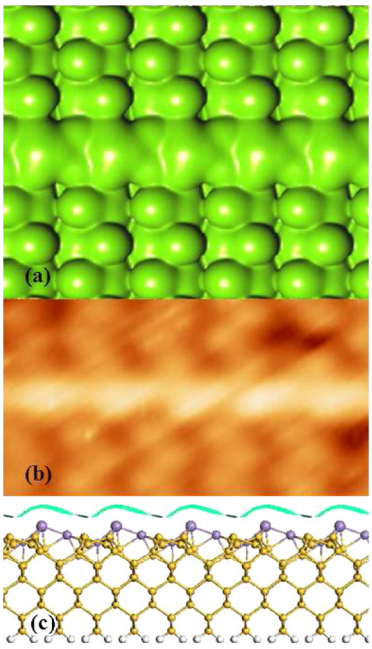

FIG. 4 (color online). (a) Simulated STM images of Mn wire on Si(001). (b) Experimental STM images [3]. (c) Side view of STM images and atomic structure, which has been matched up to the STM cross section. The model and the STM match extremely well.

We have simulated STM image for Mn wire on (2×8)-Si(001) surface. The results are in good agreement with the experimental STM image reported by Liu and Reinke [3] (see Fig. 4). Here the Mn adatom on *P* site is embedded in the surface dimer row, thus cannot be resolved, and the dimerlike Mn-Mn over the trough are distinctly buckled, exhibiting an elliptical shape in the STM images.

The formation of nanoscale wires or lines has been widely observed for different elements on Si surfaces, including the double-core 5-7-5 Bi nanolines [28,29], *PMPM* and *MMMM* dimerlike linear chains for group III and IV elements on Si(001) [24–27]. We have examined possible structures including the single-core and double-core odd-membered ring structures for Mn wires on Si(001) and found that they are all less stable.

In summary, we have performed first-principles calculations on the formation of monoatomic Mn wires on Si(001). We find that Mn adatoms prefer forming finite magic $(3n + 1)$-atom dense-linear chains perpendicular to the surface dimer rows, which is likely driven by an anisotropic selective bonding process. The chain length is limited by a competing process to form three-dimensional five-atom clusters on the substrate dimer row. The placement and bonding of Mn atoms to the Si surface is not only important to the growth mode, but also determines the magnetic properties of the assembly.

This study was supported by the NSFC of China (Grant No. 10974230) and the CAS (Grant No. KJCX2-YW-W22). C. F. C. acknowledges support by DOE under Cooperative Agreement No. DE-FC52-06NA27684. We are thankful to the crew of the Center for Computational Materials Science at IMR, Tohoku University for their support at the SR11000 supercomputing facilities.

*wjt@aphy.iphy.ac.cn

[1] M. Bolduc *et al.*, Phys. Rev. B **71**, 033302 (2005).
[2] M. C. Qian *et al.*, Phys. Rev. Lett. **96**, 027211 (2006).
[3] H. Liu and P. Reinke, Surf. Sci. **602**, 986 (2008)
[4] H. Wu, M. Hortamani, P. Kratzer, and M. Scheffler, Phys. Rev. Lett. **92**, 237202 (2004).
[5] H. Wu, P. Kratzer, and M. Scheffler, Phys. Rev. B **72**, 144425 (2005).
[6] H. Wu, P. Kratzer, and M. Scheffler, Phys. Rev. Lett. **98**, 117202 (2007).
[7] M. Hortamani, H. Wu, P. Kratzer, and M. Scheffler, Phys. Rev. B **74**, 205305 (2006).
[8] G. M. Dalpian, A. J. R. da Silva, and A. Fazzio, Phys. Rev. B **68**, 113310 (2003).
[9] G. M. Dalpian, A. J. R. da Silva, and A. Fazzio, Surf. Sci. **566-568**, 688 (2004).
[10] M. R. Krause *et al.*, Phys. Rev. B **75**, 205326 (2007).
[11] W. Zhu, H. H. Weitering, E. G. Wang, E. Kaxiras, and Z. Zhang, Phys. Rev. Lett. **93**, 126102 (2004).
[12] G. Kresse and J. Furthmüller, Phys. Rev. B **54**, 11 169 (1996); G. Kresse and J. Hafner, *ibid.* **47**, 558 (1993).
[13] P. E. Blöchl, Phys. Rev. B **50**, 17 953 (1994); G. Kresse and D. Joubert, Phys. Rev. B **59**, 1758 (1999).
[14] J. P. Perdew, K. Burke, and M. Ernzerhof, Phys. Rev. Lett. **77**, 3865 (1996).
[15] The implementations of the climbing image nudged elastic band and the dimer method for VASP were obtained from http://theory.cm.utexas.edu/henkelman.
[16] G. Brocks, P. J. Kelly, and R. Car, Phys. Rev. Lett. **66**, 1729 (1991).
[17] Y. Kamon *et al.*, Physica (Amsterdam) **308–310B**, 391 (2001).
[18] Note that use of a small (2×2) surface model can lead to surface reconstruction and the formation of interstitial Mn with a small barrier of 0.38 eV, which is similar to that reported in Ref. [7].
[19] G. Brocks and P. J. Kelly, Phys. Rev. Lett. **76**, 2362 (1996).
[20] B. Borovsky, M. Krueger, and E. Ganz, Phys. Rev. Lett. **78**, 4229 (1997).
[21] Y. W. Mo, B. S. Swartzentruber, R. Kariotis, M. B. Webb, and M. G. Lagally, Phys. Rev. Lett. **63**, 2393 (1989).
[22] Z. Zhang and Max G. Lagally, Science **276**, 377 (1997).
[23] J. T. Wang *et al.*, Phys. Rev. Lett. **97**, 046103 (2006); Phys. Rev. B **78**, 073403 (2008).
[24] X. R. Qin, F. Liu, B. S. Swartzentruber, and M. G. Lagally, Phys. Rev. Lett. **81**, 2288 (1998).
[25] E. Z. Liu *et al.*, J. Phys. Condens. Matter **20**, 445002 (2008).
[26] G. Brocks, P. J. Kelly, and R. Car, Phys. Rev. Lett. **70**, 2786 (1993).
[27] M. A. Albao *et al.*, Phys. Rev. B **72**, 035426 (2005).
[28] J. H. G. Owen, K. Miki, H. Koh, H. W. Yeom, and D. R. Bowler, Phys. Rev. Lett. **88**, 226104 (2002).
[29] J. T. Wang *et al.*, Phys. Rev. Lett. **94**, 226103 (2005).